


Photocatalytic Activity of Zinc Oxide Nanoparticles and Boric Acid for Bleaching Process on Cotton Fabric

Zeynep Ciğeroğlu¹  0000-0001-5625-6222

Zeynep Omerogullari Basyigit²  0000-0002-1526-8662

¹Uşak University, Faculty of Engineering and Natural Sciences, Department of Chemical Engineering, 64300, Uşak, Türkiye

²Bursa Uludağ University, Department of Textile, Clothing, Footwear and Leather, Textile Technology, Vocational School of Higher Education of Inegöl, 16059, Bursa, Türkiye

Corresponding Author: Zeynep Omerogullari Basyigit, zeynepbasyigit@uludag.edu.tr

ABSTRACT

In this study, a photocatalytic process was applied as an alternative to conventional hydrogen peroxide bleaching on 100% cotton fabric. The effects of ZnO nanoparticles and boric acid as catalysts were investigated. Additionally, the synergistic impact of boric acid on the well-known bleaching effect of titanium dioxide nanoparticles was explored. Unlike existing literature, the study uniquely addressed whether the photocatalytic process, without the use of any catalyst, has a specific effect, particularly in whitening, on the color spectrum. All conducted photocatalytic processes on cotton fabrics were compared with conventional hydrogen peroxide bleaching in terms of color spectra (CIE L*, a*, b*, whiteness indexes) besides the SEM, SEM-EDX, and FTIR-ATR characterization tests. Moreover, XRD, SEM, and FTIR-ATR analysis results of ZnO nanoparticles were also shared in this study. After the photocatalytic processes, tearing strength of all cotton fabrics were tested. This research is believed to shed light on future studies by evaluating more environmentally friendly pre-treatment processes in textile industry.

ARTICLE HISTORY

Received: 28.11.2023

Accepted: 08.08.2024

KEYWORDS

Photobleaching, Cotton, Zinc Oxide Nanoparticles, Boric Acid

1. INTRODUCTION

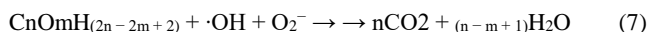
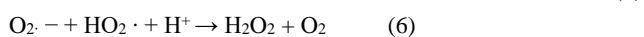
Cotton is one of the most widely used and important natural fibers in the textile industry. It comes from the fibers surrounding the seeds of the cotton plant (*Gossypium*), and it has been used for thousands of years to produce a variety of textiles. Even though cotton's versatility, comfort, and natural properties (breathability, absorbency, comfort etc.) make it a popular choice for a wide range of textile products, including apparel, home furnishings, and industrial uses; it also comes with certain disadvantages, particularly in its untreated and unprocessed form. Some of the drawbacks associated with raw cotton are being contaminated with impurities such as dust, dirt, plant material, seeds; lack of uniformity which can be varied in terms of fiber length, fineness, color; presence of natural waxes and oils can affect the wettability, dyeing process and the overall quality of the finished product [1,2]. Bleaching is a crucial process in the textile industry that involves treating raw cotton or cotton fabric with chemicals to remove impurities, natural color, and other contaminants. The goal is to achieve a clean, white appearance and

prepare the cotton for dyeing or further processing. Common bleaching agents include hydrogen peroxide, sodium hypochlorite, or chlorine dioxide [3]. Hydrogen peroxide is considered an environmentally friendly bleaching agent compared to chlorine-based alternatives. However, there are some disadvantages of using hydrogen peroxide in the finishing processes such as energy consumption because of high temperatures, pH and temperature sensitivity (higher temperatures generally increase the bleaching rate, but excessive heat may lead to fiber damage) and limited bleaching speed besides post-processing such as stabilization which increases the water consumption overall [4-6]. Researchers are constantly exploring and developing new bleaching agents to improve the efficiency, environmental sustainability, and versatility of the bleaching process in the textile industry. Photocatalysts, such as titanium dioxide, are materials that can accelerate chemical reactions under the influence of light. They are being investigated for their potential to enhance bleaching processes, particularly in the presence of ultraviolet (UV) light. When the photocatalyst absorbs

To cite this article: Ciğeroğlu Z, Omerogullari Basyigit Z. 2024. Photocatalytic Activity of Zinc Oxide Nanoparticles and Boric Acid for Bleaching Process on Cotton Fabric. *Tekstil ve Konfeksiyon*, 34(4), 454-466.

light, it creates electron-hole pairs. These charged particles can react with water and oxygen in the surrounding environment to generate reactive oxygen species (ROS), such as hydroxyl radicals ($\cdot\text{OH}$) and superoxide ions ($\text{O}_2^{\cdot-}$). The ROS generated by the photocatalyst can break down organic contaminants, pigments, and other impurities present in the textile fibers. The oxidative reactions lead to the degradation of color molecules and the removal of undesired substances. The photocatalytic process on textiles involves treating textile materials with photocatalysts and exposing them to light to achieve various effects, such as self-cleaning, antibacterial and antifungal properties [7-9].

Zinc oxide nanoparticles (n-ZnO) are commonly used in the textile industry for various purposes due to its unique properties. One of the primary uses of its in textiles is as a UV blocker. Finishing textiles with zinc oxide nanoparticles provides the fabric with enhanced UV-blocking properties. This is especially important in outdoor clothing, swimwear, and other textiles where protection from the sun's harmful ultraviolet (UV) rays is desirable. Zinc oxide has inherent antibacterial and antifungal properties. Treating textiles with zinc oxide nanoparticles can impart these properties to the fabric. This is particularly beneficial in applications where maintaining hygiene and preventing microbial growth are essential, such as in medical textiles or sportswear. In the medical field, zinc oxide nanoparticles have been incorporated into textiles to aid in wound healing. The antimicrobial properties of zinc oxide can help prevent infections in wounds. Zinc oxide nanoparticles can be incorporated into textile fibers or coatings to create nanocomposites. This integration can improve the mechanical, thermal, electroconductive and antimicrobial properties of the textiles [10-14]. The ZnO photocatalysis mechanism for cotton bleaching shown in Eq. (1-7) [15, 16].



Boric acid, a weak acid with antifungal and insecticidal properties, is sometimes used in the textile industry for specific purposes. Boric acid can be used as a flame retardant on textiles. When applied to fabrics, it forms a protective layer that helps reduce the flammability of the material. This is particularly important for textiles used in applications where fire safety is a concern. Due to its antifungal properties, boric acid can be employed as an antimicrobial treatment for textiles. Boric acid is known for its insecticidal properties, and it can be used as an insect repellent on textiles. In textile conservation, boric acid may be used as a preservative to protect historical textiles from

decay and insect damage [17-21]. Boron doping is known to enhance photocatalytic activity under visible light by reducing the bandgap between the photogenerator and the photocatalyst [22-24]. In accordance with the above data, we have used it to whiten cotton material under UV-A light to determine whether boric acid has a direct effect. To the best of our knowledge and based on the literature, this study is the inaugural investigation into the photochemical bleaching process on cotton fiber using ZnO nanoparticles and boric acid under UV-A source. This study diverges from existing literature by exploring an alternative approach to the conventional bleaching process for untreated cotton fabrics. The focus is on investigating the photocatalytic bleaching effects of boric acid and zinc oxide nanoparticles on raw cotton fabrics. Additionally, the study delves into the synergistic impacts on whiteness indexes when boric acid is combined with titanium dioxide nanoparticles (n-TiO₂), renowned for their nano-sized bleaching effects. One distinctive aspect of this article compared to many other photocatalytic textile studies in the literature is the exploration of the impact of the photocatalysis process itself on bleaching, without the use of any catalyst.

2. MATERIAL AND METHOD

2.1 Material

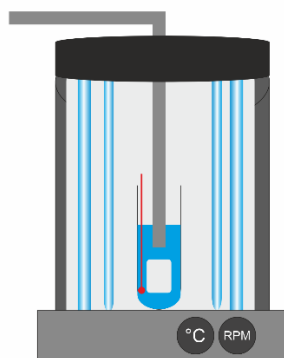
Boric acid (99.8%) was supplied from Alfa Aesar. NaOH and HCl were purchased from Sigma Aldrich. ZnO (99.99%, 18 nm) and TiO₂ (99.99%, 28 nm, anatase) supplied from Nanografi, Turkey. The technical specifications of the ZnO nanoparticles, TiO₂ nanoparticles, H₃BO₃ were detailed in Table 1. In our experimental investigations, 100% woven cotton fabrics (weighing 145 g/m²) consisting of Ne 20/1 fine yarns were sourced from Ege Özteks Tekstil, located in Uşak, Turkey. To conduct the pre-treatment procedures, we acquired alpha-amylase desizing enzyme, NaOH (48 Bé), and a wetting agent from Alfa Kimya, Turkey.

2.2 Method

As part of the pre-treatment phase, following the desizing procedure conducted using a pad-batch machine (Babkok) with an 80% wet-pick-up ratio employing 2g/L of alpha-amylase desizing enzyme and 1 g/L of wetting agent, a solution of 30 g/L NaOH (48 Bé) was applied to the cotton fabrics using the same machine. This step aimed to boost the hydrophilicity of the materials, as per the industrial standards of the supplier company (Ege Özteks Tekstil). The homemade photocatalytic system is shown in Figure 1. There are 15 Watt UV-A lamps (Osram L Blue UVA L 15W/78) each in the system and the system is galvanised. The system was previously homemade and its shape was shown in the previous publication [25].

Table 1. Technical Properties of n-ZnO, n-TiO₂ and Boric acid

Technical data of ZnO				
Purity (%)	99.5			
Average Particle Size (nm)	18			
Morphology	nearly spherical			
Color	white			
Specific Surface Area (m ² /g)	20.0-65.0			
Crystal Phase	single crystal			
True Density (g/cm ³)	5.5			
Elemental Analysis (%)	Mn	Cu	Pb	
	0.0002	0.0004	0.001	
Technical data of n-TiO ₂				
Purity (%)	99.995			
Average Particle Size (nm)	28			
Color	white			
Specific Surface Area (m ² /g)	55.00			
pH	5.5-6.5			
True Density (g/cm ³)	4.1			
Elemental Analysis (%)	K	Na	Fe	Al
	0.0055	0.0053	0.003	0.0022
Technical Data of Boric acid				
Melting point	ca. 185° deg.			
Density	1.435			
Form	+ 8 mesh granular			

**Figure 1.** The illustration of homemade photocatalytic system [25].

The fabrics cut in certain sizes were placed in a 250 mL beaker and the experimental conditions given in Table 2 were applied.

Table 2. Experimental Set-up

Sample Code	Finishing Process
S1	Untreated fabric
S2	n-ZnO 1 g/L pH 10.5 60 C 60 min
S3	n-ZnO 5 g/L pH 10.5 60 C 60 min
S4	n-ZnO 5 g/L pH 4.5 60 C 60 min
S5	n-ZnO 5 g/L pH 7 60 C 60 min
S6	n-ZnO 5 g/L pH 4.5 30 C 60 min
S7	n-ZnO 5 g/L pH 10.5, 95 C 60 min
S8	Boric acid/n-TiO ₂ (2.5+2.5) g/L pH 5.5 60 C 60 min
S9	Boric acid 5g/L pH 5.5 60 C 60 min
S10	Without catalyst 30 C 60 min pH 7
S11	Without catalyst 60 C 60 min pH 7
S12	Without catalyst 95 C 60 min pH 7
S13	Conventional bleaching process

2.3. Performance and characterization tests of the materials

In order to ascertain the crystallographic phase of the specimens, an X-ray diffractometer (Malvern Panalytical, Netherlands) employing Cu K α radiation was utilized. The diffraction patterns were scrutinized within a range spanning from 10 to 90°. Microstructural variations within the materials were examined using a field emission scanning electron microscope (SEM) equipped with elemental analysis via SEM-EDX, model XL-30 SFEG, produced by Philips in Eindhoven, Netherlands. Prior to SEM imaging, the specimens were subjected to Au coating to enhance conductivity. Fourier Transform Infrared Spectroscopy (FTIRS) spectra for cotton specimens were acquired using a Spectrum Two FTIR spectrophotometer. Alongside the aforementioned characterization tests, color spectrum analysis and tearing strength evaluations were conducted on the cotton samples. CIELAB color spectrum results, incorporating parameters such as L*, a*, b*, whiteness and yellowness indexes and ΔE were determined using a Konica Minolta CM-3600D Spectrophotometer from Japan. Tearing strength assessments on cotton samples, in both warp and weft directions, were carried out in accordance with Elmendorf ASTM D1424 standards. The tear strengths were measured utilizing a D-type pendulum with a weight of 64 N.

3. RESULTS AND DISCUSSION

3.1 Characterization Results of ZnO nanoparticles, H₃BO₃ and TiO₂ nanoparticles

3.1.1. FTIR of ZnO nanoparticles, H₃BO₃ and TiO₂ nanoparticles

Zinc oxide nanoparticles (ZnO-n) exhibited vibrations in the 420-600 cm^{-1} range, which correspond to Zn-O stretching vibrations in the 434 cm^{-1} range [26], as mentioned in our previous publication [27] (Figure 2). The distinctive peak of the B-O bond is 1430 cm^{-1} , whereas the stretching vibration of the intermolecular hydrogen bond (O-H) is 3200 cm^{-1} , whereas the O-H surface curvature at 699 cm^{-1} [28]. The transmittance peaks, spanning from 600 to 850 cm^{-1} , are associated with the Ti-O-Ti links seen in TiO_2 nanoparticles (n- TiO_2) [29]. The unique band corresponding to anatase titania was observed at 745 cm^{-1} in the FTIR spectra of pure n- TiO_2 [30]. In the FTIR spectra of the pure n- TiO_2 , a noticeable stretching peak at 1640 cm^{-1} indicates the stretching of Ti-OH [30]. It was determined that the big peak at 3305 cm^{-1} was caused by the stretching vibration of the -OH group.

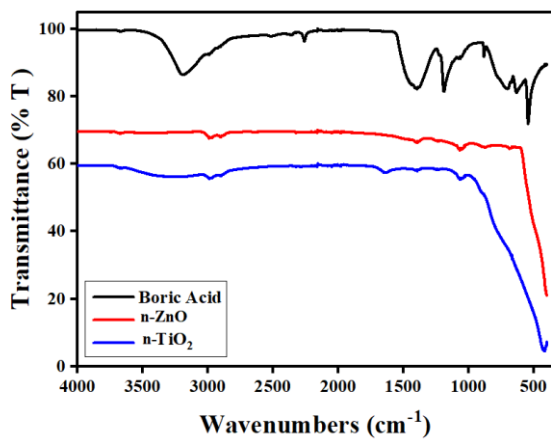


Figure 2. FTIR graph of n-ZnO, H_3BO_3 and n- TiO_2

3.1.2 . XRD analysis of ZnO nanoparticles, H_3BO_3 and TiO_2 nanoparticles

Zinc oxide nanoparticles with 2θ values of 31.71, 34.58, 36.20, 47.53, 56.65, 62.88, 66.47, 67.96, and 69.34 degrees are evident, as previously mentioned in our published paper

[31]. XRD pattern of ZnO obtained from Nanografi agrees with JCPDS Data Card No. 36-1451 (Figure 3). The main signal was seen in XRD pattern of boric acid at 28.00° [32]. The primary peaks are seen in the XRD patterns of the boric acid (H_3BO_3) card number, ICDD-00-030-0620 [33]. The anatase peaks (JCPDS Card no. 21-1272) at 2θ values of 25.31, 37.81, 48.05, 53.91, 55.06, and 62.68 are displayed in Figure 3 [25, 34]. The anatase structure is clearly indicated by these peaks.

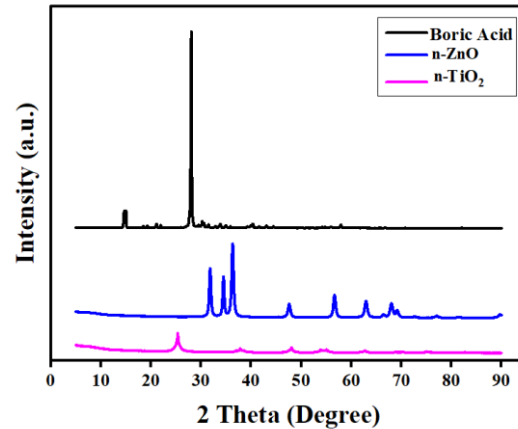
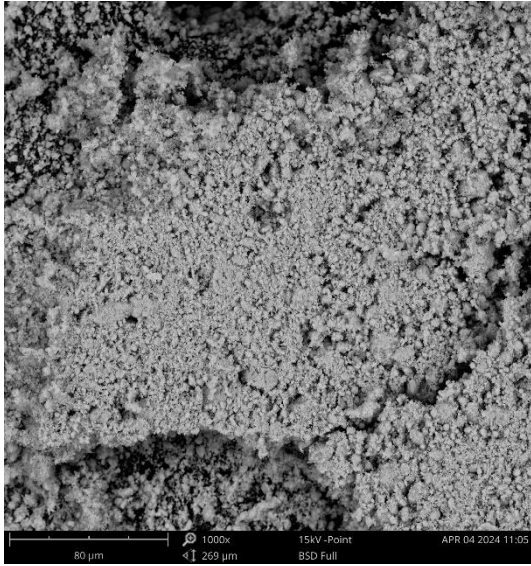


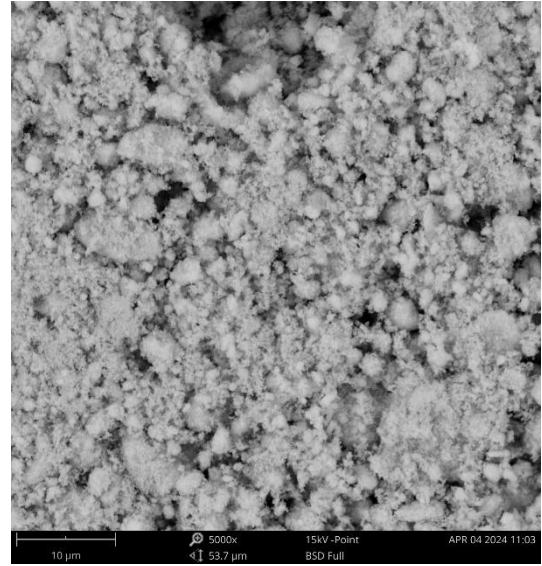
Figure 3. XRD patterns of n-ZnO, H_3BO_3 and n- TiO_2

3.1.3. SEM analysis of ZnO nanoparticles, H_3BO_3 and TiO_2 nanoparticles

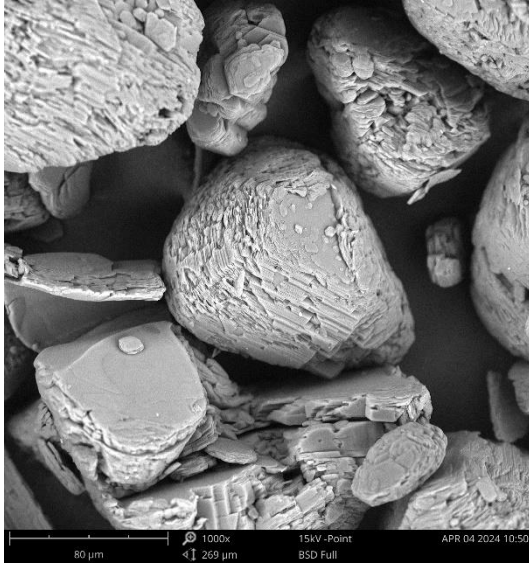
Based on the SEM image (Figure 4), the majority of the ZnO nanopowder displayed a spherical morphology with a minor rod shape [35]. Boric acid has a surface that is essentially flat and roughened by fibrils, according to SEM observation [36]. Upon closer examination, the 500 nm SEM picture in Figure 4 clearly resembles a cauliflower [37]. This study shows that the anatase form of n- TiO_2 adopts a structure with several anatase nanoparticle microspheres, like a hierarchical cauliflower.



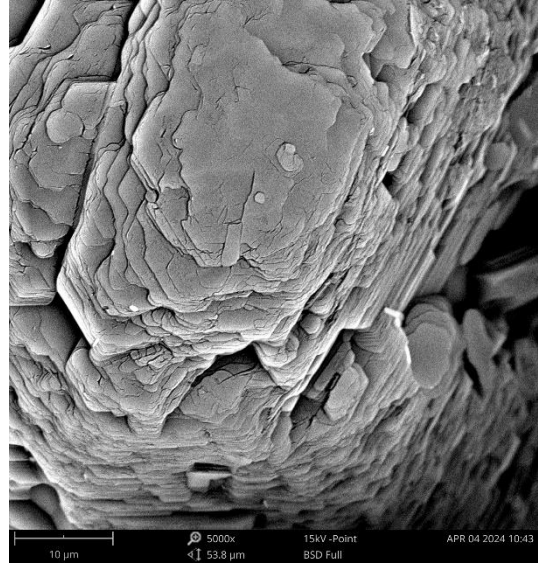
a) n-ZnO X1000



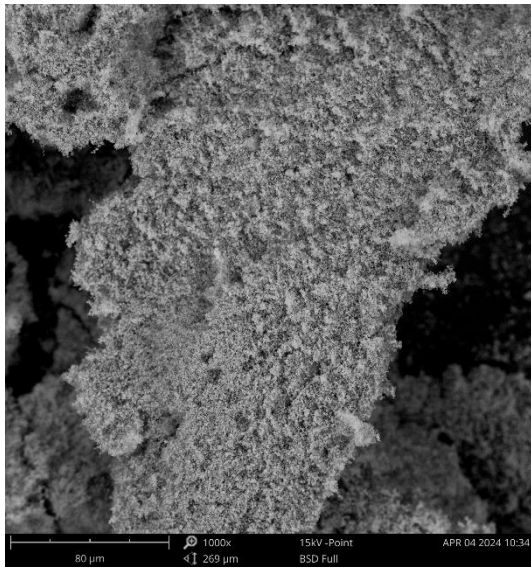
b) n-ZnO X5000



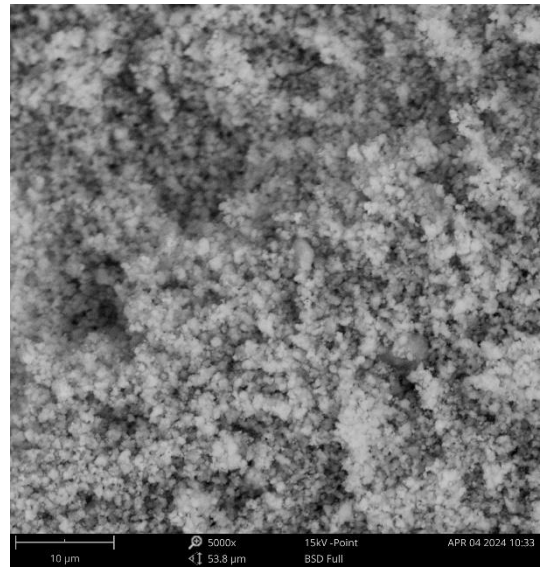
c) Boric acid X1000



d) Boric acid X5000



e) n-TiO₂ X1000

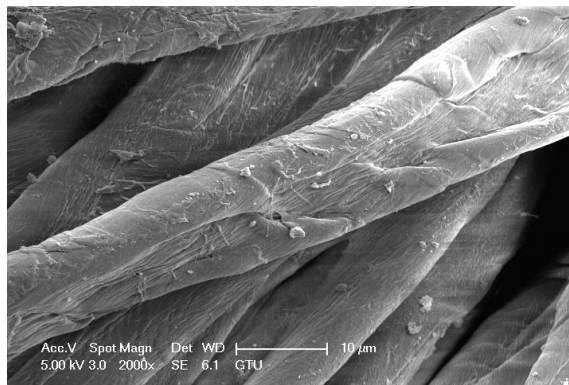


f) n-TiO₂ X5000

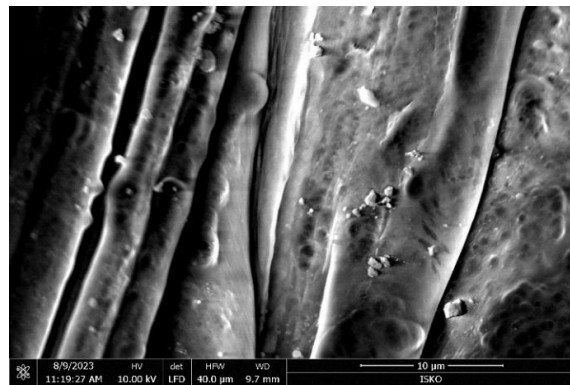
Figure 4. SEM image of n-ZnO powder, n-TiO₂ powder and boric acid.

3.2. Characterization Results of Fabric Samples

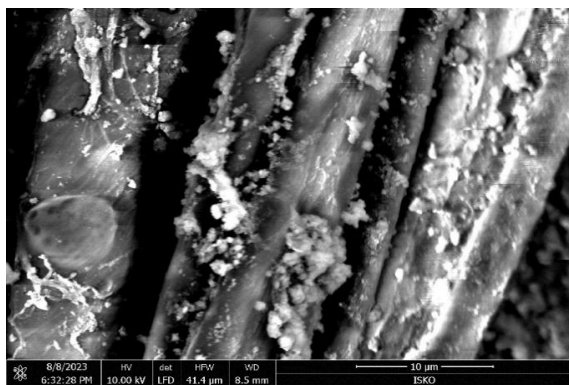
3.2.1. SEM Results of Cotton Fabric



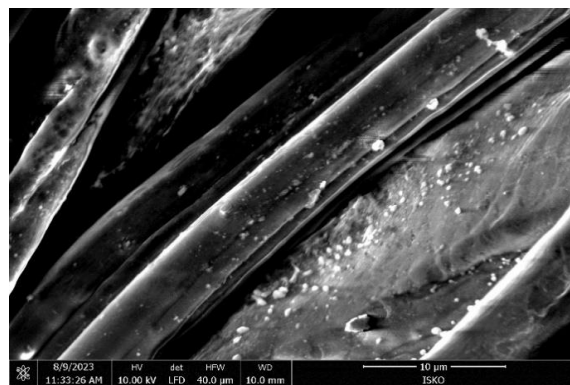
a) S1x 2000



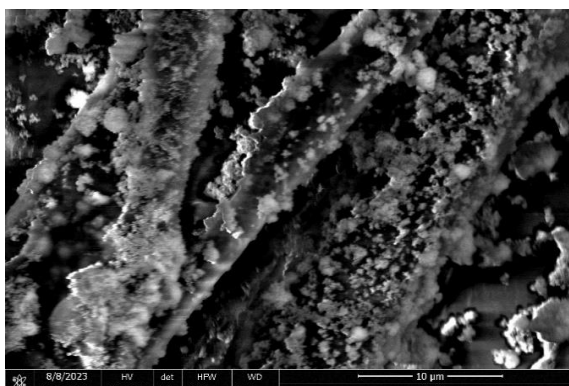
b) S11 X2000



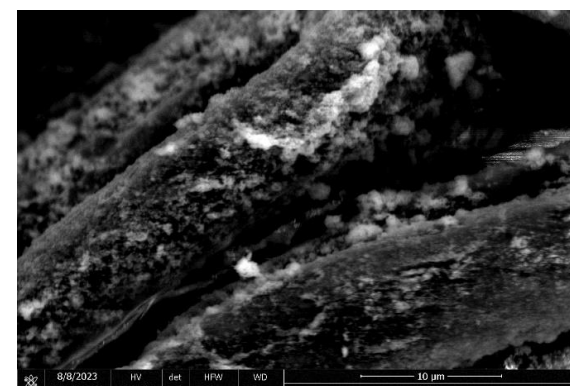
c) S8 x2000



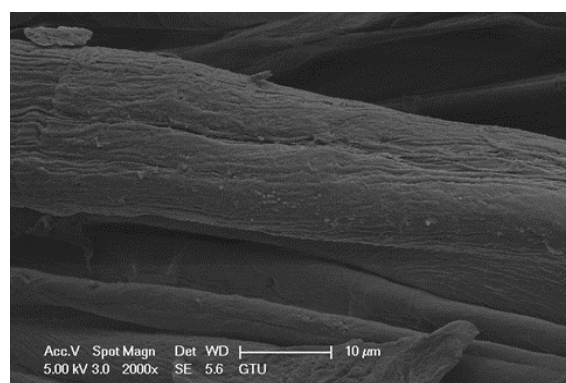
d) S9 X2000



e) S3 X2000



f) S5x2000



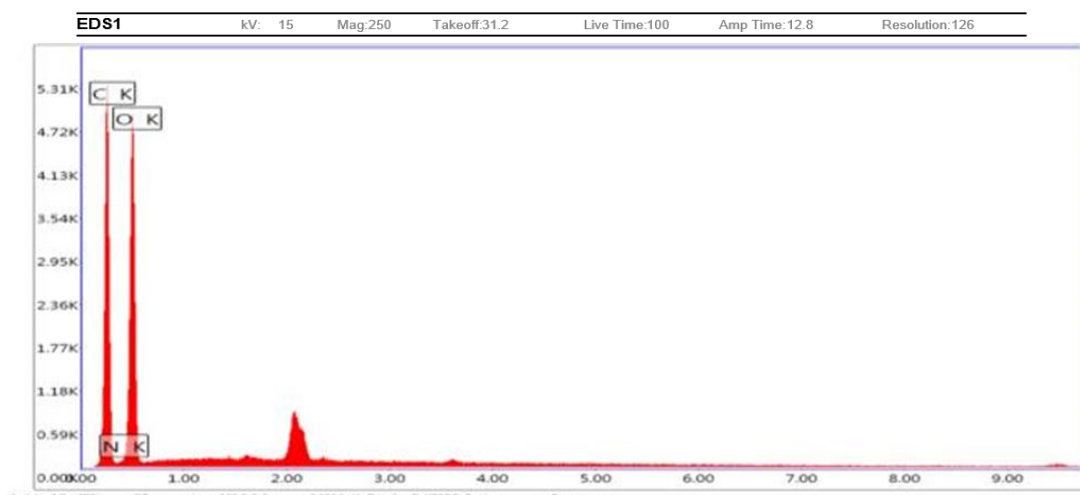
g) S13 X2000

Figure 5. SEM pictures of untreated and treated cotton fabrics

Figure 5 displays SEM images of both untreated and treated cotton fabrics. In Figure 5.a, the surface of the untreated cotton fabric appears clear and smooth. In Figure 5.b, on the other hand, fluctuations and pits are evident on the surface of cotton fabric subjected to photocatalytic treatment without any catalyst used, as indicated. It is presumed that this effect is a result of the impact of UV rays used in the photocatalytic process on the surface. The SEM micrograph in Figure 5.d depicts a cleaner surface compared to Figure 5.c. This can be attributed to the fact that in S9, only the cotton surface treated with boric acid is

present, while the sample in S8 undergoes treatment with TiO₂ nanoparticles and boric acid. The particles observed in S8 belong to n-TiO₂. Figs.5.e and 5.f showcase the fiber surfaces of cotton fabrics treated with ZnO nanoparticles at pH 10.5 and pH 7, respectively. ZnO nanoparticles are distinctly visible in both micrographs. In the final figure, Fig.5g, the micrograph illustrates a conventionally hydrogen peroxide-bleached raw cotton fabric. Unlike all other figures, it is apparent that this treatment causes abrasions on the fiber surface and damages the fibers.

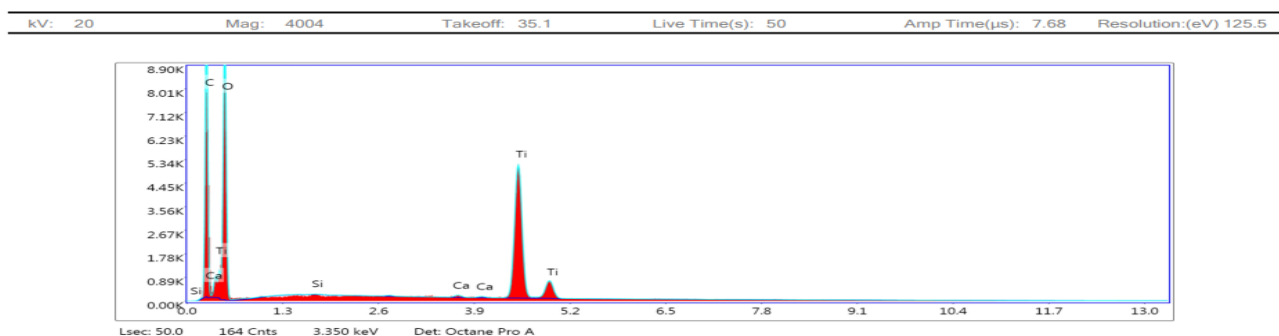
3.2.2. SEM-EDX Results of Cotton Fabric



a) SEM-EDX analysis of S1

Element	W %	Atomic	Net Int.	Net Int. Error
C K	45.2	52.17	288.41	0.01
N K	2.74	2.71	3.93	0.11
O K	52.06	45.12	289.84	0.01

b) SEM-EDX analysis of S1 table 2

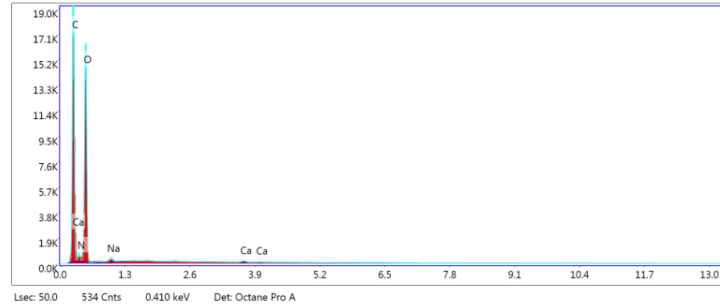


eZAF Smart Quant Results

Element	Weight %	Atomic %	Net Int.	Error %	Kratio	Z	A	F
C K	32.91	44.49	884.52	6.57	0.1757	1.0664	0.5008	1.0000
O K	48.43	49.16	974.13	9.86	0.0784	1.0209	0.1586	1.0000
Si K	0.02	0.01	1.91	76.01	0.0001	0.9285	0.7533	1.0058
Ca K	0.26	0.10	21.07	15.43	0.0025	0.8768	1.0181	1.0730
Ti K	18.39	6.23	1224.81	2.05	0.1517	0.7948	1.0247	1.0133

c) SEM-EDX analysis of S8

kV: 20 Mag: 4004 Takeoff: 35.2 Live Time(s): 50 Amp Time(µs): 7.68 Resolution:(eV) 125.5

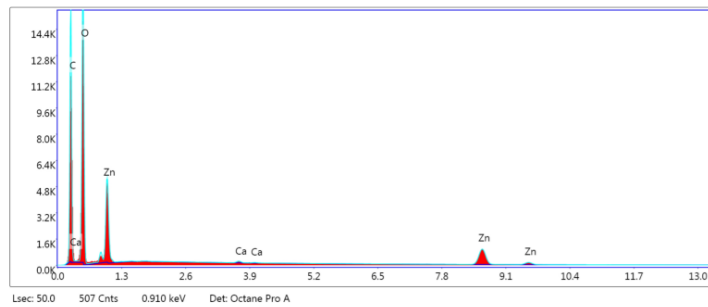


eZAF Smart Quant Results

Element	Weight %	Atomic %	Net Int.	Error %	Kratio	Z	A	F
C K	45.86	52.89	1945.57	5.59	0.2714	1.0239	0.5777	1.0000
N K	3.92	3.88	50.04	34.03	0.0047	0.9995	0.1188	1.0000
O K	49.47	42.83	1692.83	9.37	0.0958	0.9784	0.1978	1.0000
NaK	0.55	0.33	35.23	15.87	0.0017	0.8873	0.3575	1.0009
CaK	0.20	0.07	21.77	18.00	0.0018	0.8362	1.0306	1.0477

d) SEM-EDX analysis of S9

kV: 20 Mag: 4004 Takeoff: 35.2 Live Time(s): 50 Amp Time(µs): 7.68 Resolution:(eV) 125.5

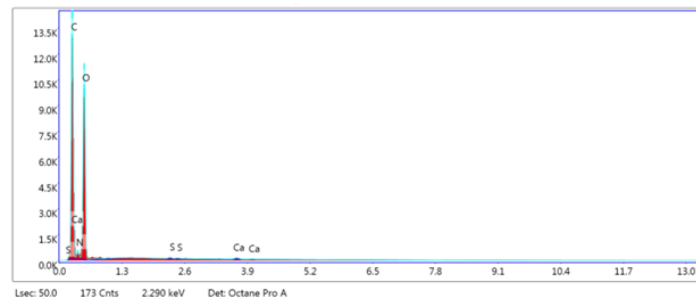


eZAF Smart Quant Results

Element	Weight %	Atomic %	Net Int.	Error %	Kratio	Z	A	F
C K	43.12	53.93	1319.68	7.30	0.1874	1.0468	0.4153	1.0000
O K	46.49	43.65	1757.71	9.13	0.1012	1.0016	0.2174	1.0000
CaK	0.22	0.08	23.73	21.14	0.0020	0.8595	1.0105	1.0373
ZnK	10.17	2.34	313.65	3.63	0.0810	0.7307	1.0159	1.0732

e) SEM-EDX analysis of S3

kV: 20 Mag: 4004 Takeoff: 35 Live Time(s): 50 Amp Time(µs): 7.68 Resolution:(eV) 125.5



eZAF Smart Quant Results

Element	Weight %	Atomic %	Net Int.	Error %	Kratio	Z	A	F
C K	47.21	54.21	1462.88	5.60	0.2824	1.0231	0.5845	1.0000
N K	3.63	3.58	32.50	47.88	0.0042	0.9986	0.1153	1.0000
O K	48.81	42.08	1181.77	9.52	0.0923	0.9775	0.1935	1.0000
S K	0.09	0.04	10.92	24.89	0.0008	0.8675	0.9605	1.0121
CaK	0.25	0.09	20.25	20.72	0.0023	0.8355	1.0313	1.0476

f) SEM-EDX analysis of S13

Figure 6. SEM-EDX analysis of untreated and treated cotton fabrics

Figure 6 showcases the SEM-EDX analysis results for both treated and untreated cotton fabrics. In Figure 6a, the untreated cotton fabric and Fig. 6b, where no catalyst was used, prominently exhibit the presence of C and O elements. Moving to Fig. 6c, the photocatalytic process with the introduction of titanium dioxide nano particles in the process reveals a 18.39% presence of Ti element. Fig. 6d, on the other hand, depicts a photocatalytic process applied solely with boric acid. Since boric acid, unlike nano materials, does not increase surface roughness (refer to SEM micrographs) and spreads on the surface, it could not be captured elementally in SEM-EDX analysis. In addition, the inconspicuous appearance of the boron element in SEM-EDX analysis is attributed to boron's low atomic number, which results in its inability to generate X-ray fluorescence signals. Furthermore, the detection is complicated by the fact that boron's characteristic X-ray spectral lines are weaker compared to other elements.

However, in Fig. 6e, the SEM-EDX analysis of cotton fabric exposed to photocatalytic treatment with 5 g/L ZnO nanoparticles at pH 10.5 for 60 minutes at 60 C reveals the presence of 10.17% Zn element in addition to the dominant C and O elements. The last figure illustrates the SEM-EDX analysis of conventionally hydrogen peroxide-treated cotton fabric. The hydrogen molecule, because of being very small, could not be captured in the elemental analysis, but the presence of the other basic elements that make up the cotton fibers (carbon and oxygen) has been demonstrated.

3.2.3. FTIR-ATR Analysis of Cotton Fabric

In Figure 7, FTIR-ATR spectra of untreated cotton fabric, conventionally hydrogen peroxide-bleached fabric, fabric subjected to photocatalytic treatment without any catalyst, fabric treated with a combination of boric acid and TiO₂ nanoparticles in a photocatalytic process, fabric treated solely with boric acid in a photocatalytic process, and fabric subjected to photocatalytic treatment with 5 g/L ZnO nano particles under the same conditions are sequentially presented. The characteristic peaks of cotton are discernible in the graph. When the FTIR-ATR analysis of the untreated fabric was examined, distinctive peaks associated with cotton fibers were observed at the following wavenumbers: 3300 cm⁻¹ (OH stretching), 1030 cm⁻¹ (CO stretching), 2900 cm⁻¹ (CH stretching), and 1310 cm⁻¹ (CH vibration). However, the FTIR spectras for both untreated and treated cotton fabrics are overlapped. This is attributed to the inorganic nature of the catalysts and chemical agents, such as n-ZnO, n-TiO₂, boric acid, and hydrogen peroxide, and their usage in relatively low proportions.

3.3. Color Spectrum Results

Table 3 provides the whiteness indexes (Berger) and yellowness indexes (ASTMD1925) along with CIE L*, a*, b* and ΔE values for untreated and treated cotton fabrics. According to this table, it is observed that photocatalytic

processes with zinc oxide nano particles at different pH levels and temperatures slightly increased the whiteness index values. Among the processes conducted with nano zinc oxide, the best result was achieved with the treatment at pH 10.5 and 60C for 60 minutes. Although these values are lower compared to bleaching results obtained using different catalysts or conventional bleaching process with hydrogen peroxide, the results of zinc oxide nano particles are in line with the literature [38] In their study, Arık and Atmaca [38] utilized various zinc-based nano particles, including nano zinc oxide with sizes ranging from 10 to 30 nm, and found that Stensby whiteness ratings were consistently at similar levels (with a 3-unit increase). The 18 nm zinc oxide used in this study marginally increased whiteness values but did not result in effective bleaching. Additionally, examining the color spectrum results of photocatalytic processes with boric acid showed a slight increase in whiteness and decrease in yellowness indexes. The combination with n-TiO₂ significantly enhanced the whiteness index result whereas the yellowness indexes decreased; however, it is believed to be attributed to the high photocatalytic effect of n-TiO₂. No significant differences in ΔE values were observed for any samples processed, except for those involving the use of titanium dioxide. Unlike other photocatalytic textile applications, this study explored the impact of photocatalytic processes on bleaching without using a catalyst, revealing that the treatment conducted at pH 7 and 60 C for 60 minutes, excluding n-TiO₂, had the highest bleaching effect. In catalyst-free photocatalytic processes, the formation of whiteness is generally associated with the oxidative properties of the mechanism and the nature of the reaction. Photocatalytic processes involve catalysts that trigger and accelerate chemical reactions using light energy. However, catalyst-free photocatalytic processes typically encompass conditions where various components are directly exposed to light, leading to oxidation-reduction reactions. Whiteness often arises from the breakdown or reaction of colored pigments or organic substances. Catalyst-free photocatalytic processes, especially those involving the breakdown or degradation of organic materials and the increased solubility of color pigments, can result in the appearance of whiteness. This occurs as the impact of colored substances diminishes, allowing lighter to be reflected. These processes are commonly utilized in applications such as the removal of organic pollutants or the bleaching of materials. For example, catalyst-free photocatalytic reactions under sunlight can lead to the breakdown of colored stains or pigments, resulting in the material becoming whiter [39].

3.4. Tearing Strength Results

In Figure 8, the results of the tear strength for untreated cotton fabric, fabric subjected to conventional bleaching, fabric treated with zinc oxide nanoparticles under various conditions of photocatalytic treatment, fabric treated with boric acid and boric acid with n-TiO₂ photocatalytic

treatment, and finally, cotton fabric subjected to photocatalytic treatment without any catalyst are presented. According to Figure 8, it can be observed that the tear strength of all fabrics decreased to some extent. While the decrease caused by conventional bleaching in cotton fabric was 7.62%, this value increased to 12.7% as a result of the photocatalytic treatment with zinc oxide nanoparticles. When the amount of zinc oxide nanoparticles increased to 5 g/L, this value was observed to reach the range of 13-14%. The further increase in the decrease is thought to be due to

the accumulation of nanoparticles at the intersections and surfaces of fibers, leading to an increase in the coefficient of friction between the fibers. Moreover, while a 9.6% decrease in tear strength was observed as a result of photocatalytic treatment with boric acid alone, this decrease reached 13% when nano TiO₂ was used as a catalyst together with boric acid. It was observed that photocatalytic treatments conducted without catalysts resulted in less tear strength loss (7.99%) compared to those conducted with catalysts.

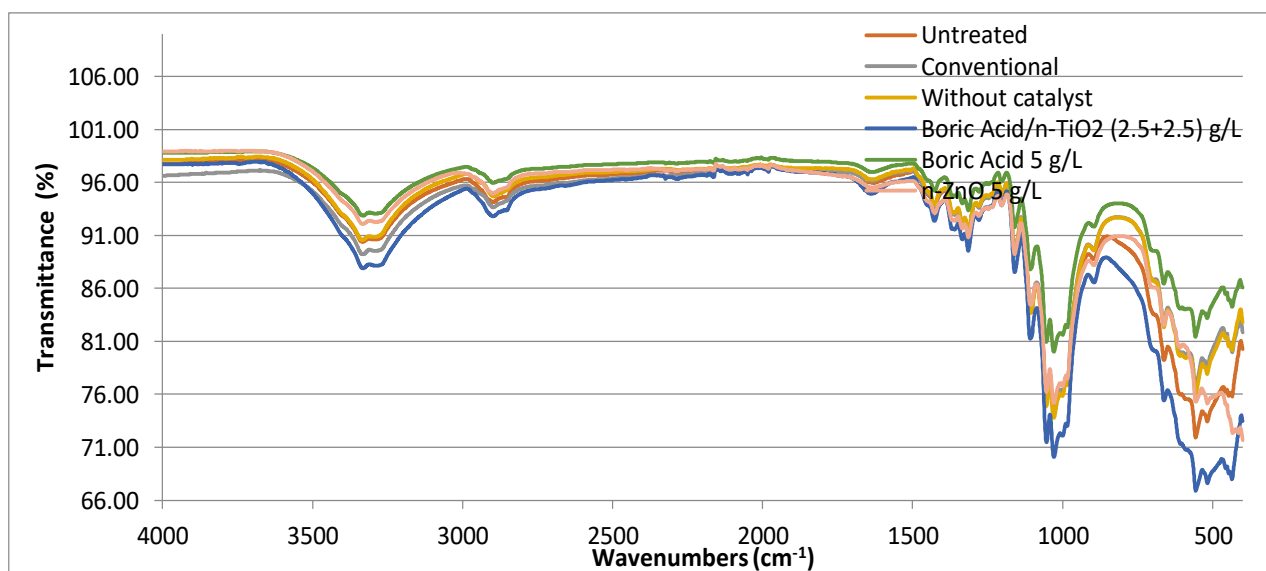


Figure 7. FTIR-ATR analysis of untreated and treated cotton fabrics

Table 3. Color spectrum values

SAMPLES		Whiteness Index-BERGER	Yellowness Index ASTMD 1925	L*	a*	b*	ΔE
S1	Untreated fabric	63.15	7.42	92.54	-0.18	4.01	-
S2	n-ZnO 1 g/L pH 10.5 60 C 60 min	64.36	7.17	92.98	-0.28	3.98	0.45
S3	n-ZnO 5 g/L pH 10.5 60 C 60 min	64.38	7.14	93.54	-0.94	4.48	1.34
S4	n-ZnO 5 g/L pH 4.5 60 C 60 min	64.12	7.29	93.73	-0.71	4.52	1.40
S5	n-ZnO 5 g/L pH 7 60 C 60 min	63.77	7.39	93.61	-1.06	4.69	1.54
S6	n-ZnO 5 g/L pH 4.5 30 C 60 min	63.12	7.38	93.36	-0.61	4.01	1.07
S7	n-ZnO 5 g/L pH 10.5 95 C 60 min	61.65	9.14	93.73	-0.94	5.14	1.81
S8	Boric acid/n-TiO ₂ (2.5+2.5)g/L pH 5.5 60C 60min	73.98	3.36	94.88	-0.18	4.01	2.64
S9	Boric acid 5g/L pH 5.5 60 C 60 min	64.84	7.20	93.00	-0.23	3.86	0.49
S10	Without catalyst 30 C 60 min pH 7	66.50	6.60	93.08	-0.21	3.52	0.328
S11	Without catalyst 60 C 60 min pH 7	66.67	6.15	93.55	-0.27	3.70	0.253
S12	Without catalyst 95 C 60 min pH 7	65.98	6.02	93.07	-0.20	3.62	0.250
S13	Conventional bleaching process	70.50	4.87	93.98	-0.36	3.12	0.832

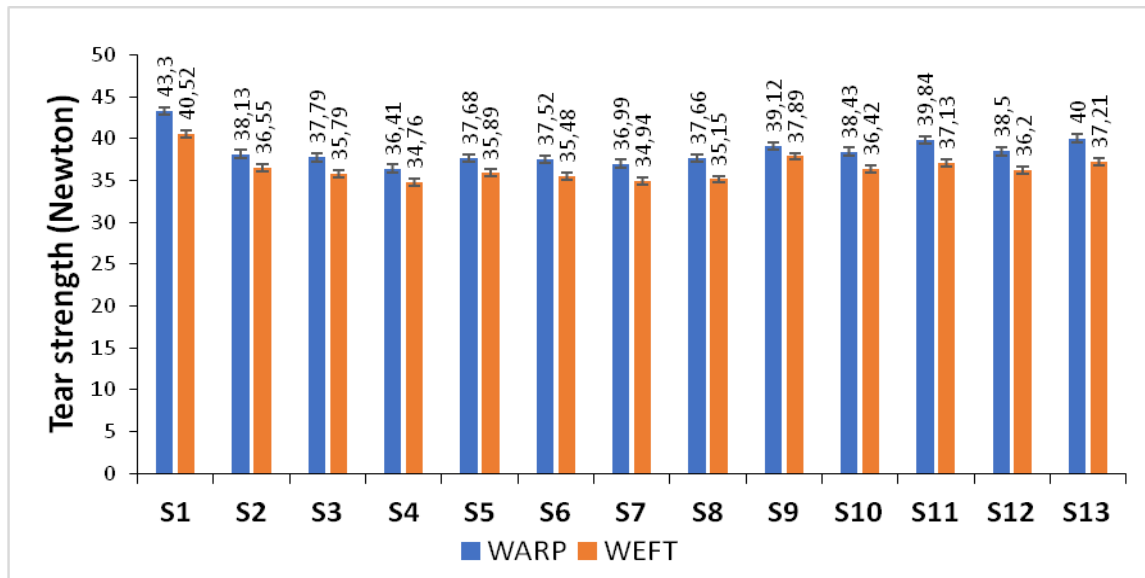


Figure 8. Tearing strenght results of cotton samples

3.5. UV intensity results

The characteristics of the lamp used are given in Table 4.

Table 4. Electrical and photometrical fata for Osram L Blue UVA L 15W/78

Electrical Data		Photometrical Data	
Nominal Voltage	55 V	Luminous Intensity	7800 cd
Lamp Voltage	55 V	Radiated Power 315...400 nm (UVA)	4 W
Construction Voltage	230 V		
Lamp Current	0.33 A		
Nominal Wattage	15 W		

Consider it endless and visualize the source as a cable. From then on, it is acknowledged that it only radiates in the form of $2\pi rL$ from the lateral field. by considering the source as an infinitely long cylinder with r near to zero and using in Eq (8) as follows;

$$I = \frac{P}{2\pi rL} \quad (8)$$

Where P is radiated power, r is radius and L is cylcinder of lengthh.

$$I = \frac{4x4}{2x\pi x0.15x0.39}$$

Thus, UV intensity of our lamps are calculated as; 43.53 W/m².

4. CONCLUSION

In this study, due to the disadvantages of conventional hydrogen peroxide bleaching for cotton fabrics, a quest for a more environmentally friendly method for bleaching was

initiated. Various catalysts were examined individually or in combination, and their effects on whiteness indexes were investigated. Characterization studies were also conducted. Unlike other textile photocatalytic studies, this research addressed the question of whether catalyst-free photocatalytic processes would induce any changes in cotton fiber surface and color performance. According to the results, zinc oxide nano particles did not provide a significant bleaching effect; however, they slightly increased whiteness indexes, with the best values observed under the parameters of a photocatalytic process conducted at 60 C, pH 10.5, and for 60 minutes. Additionally, the photocatalytic process with boric acid, although marginally, increased whiteness indexes. Catalyst-free photocatalytic processes, excluding n-TiO₂ and conventional methods, yielded the highest whiteness index. Characterization tests and elemental analyses were conducted to elucidate the impact of catalysts. In conclusion, the increase in whiteness index without the use of any chemical or catalyst suggests that it could be an alternative method to hydrogen peroxide bleaching, which involves high water and energy consumption and poses a significant environmental burden.

Acknowledgement

This study was not funded by any organisation. The authors thank Ege Özteks Tekstil for providing the cotton fabrics.

REFERENCES

1. Wang H., Siddiqui M. Q., & Memon H. (2020). Processing Physical Structure, properties and quality of cotton. Wang, H, Memon, H. Cotton science and processing technology: Gene, ginning, garment and green recycling. *Springer* 79–97.
2. Gordon S., Rodgers J., & Abidi N. (2017). Cotton fibre cross-section properties. Cotton fibres, characteristics, uses and performance, *Nova* 65–86.
3. Pereira L., Bastos C., Tzanov T., Cavaco-Paulo A., & Gübitz G. M. (2005). Environmentally friendly bleaching of cotton using laccases. *Environmental Chemistry Letters* 3, 66–69.
4. Wang N., Tang P., Zhao C., Zhang Z., & Sun G. (2020). An environmentally friendly bleaching process for cotton fabrics: mechanism and application of UV/H₂O₂ system. *Cellulose* 27(2), 1071–1083.
5. Fei X., Yao J., Du J., Sun C., Xiang Z., & Xu C. (2015). Analysis of factors affecting the performance of activated peroxide systems on bleaching of cotton fabric. *Cellulose* 22, 1379–1388.
6. Farooq A., Ali S., Abbas N., Fatima G A., & Ashraf, M A. (2013). Comparative performance evaluation of conventional bleaching and enzymatic bleaching with glucose oxidase on knitted cotton fabric. *Journal of Cleaner Production* 42, 167–171.
7. Zeghioud H., Assadi AA., Khellaf N., Djelal H., Amrane A., & Rtimi,S. (2018). Reactive species monitoring and their contribution for removal of textile effluent with photocatalysis under UV and visible lights: dynamics and mechanism. *Journal of Photochemistry and Photobiology A: Chemistry* 365, 94–102.
8. Rahal R., Pigot T., Foix D., & Lacombe S. (2011). Photocatalytic efficiency and self-cleaning properties under visible light of cotton fabrics coated with sensitized TiO₂. *Applied Catalysis B: Environmental* 104(3–4), 361–372.
9. Ashar A., Bhutta Z A., Shoaib M., Alharbi NK., Fakhar-e-Alam M., Atif M., et al. (2023). Cotton fabric loaded with ZnO nanoflowers as a photocatalytic reactor with promising antibacterial activity against pathogenic E. coli. *Arabian Journal of Chemistry* 105084.
10. Xia C., Liu S., Cui B., Li M., Wang H., Liang C. (2022). In situ synthesis of zinc oxide/selenium composite for UV blocker application. *International Journal of Applied Ceramic Technology* 19(5), 2437–2449.
11. Sirelkhatim A., Mahmud S., Seeni A., Kaus NHM., Ann LC., Bakhori SKM.(2015). Review on zinc oxide nanoparticles: antibacterial activity and toxicity mechanism. *Nano-micro letters* 7, 219–242.
12. Raghupathi KR., Koodali RT., & Manna, AC. (2011). Size-dependent bacterial growth inhibition and mechanism of antibacterial activity of zinc oxide nanoparticles. *Langmuir* 27(7), 4020–4028.
13. Miri A., Mahdinejad N., Ebrahimi O., Khatami M., & Sarani M. (2019). Zinc oxide nanoparticles: Biosynthesis, characterization, antifungal and cytotoxic activity. *Materials Science and Engineering: C* 104, 109981.
14. Singh P., & Nanda A. (2013). Antimicrobial and antifungal potential of zinc oxide nanoparticles in comparison to conventional zinc oxide particles. *J. Chem. Pharm. Res* 5(11), 457–463.
15. Montazer M., & Morshedi S. (2012). Nano photo scouring and nano photo bleaching of raw cellulosic fabric using nano TiO₂. *International Journal of Biological Macromolecules* 50(4), 1018–1025.
16. Behnajady MA., Modirshahla N., & Hamzavi R. (2006). Kinetic study on photocatalytic degradation of C.I. Acid Yellow 23 by ZnO photocatalyst. *Journal of Hazardous Materials*, 133(1), 226–232. <https://doi.org/https://doi.org/10.1016/j.jhazmat.2005.10.022>
17. Selvakumar N., Azhagurajan A.,Natarajan TS., & Mohideen Abdul KhadirM. (2012). Flame-retardant fabric systems based on electrospun polyamide/boric acid nanocomposite fibers. *Journal of applied polymer science* 126(2), 614–619.
18. Arvanitis C., Rook T., & Macreadie I. (2020). Mechanism of action of potent boron-containing antifungals. *Current Bioactive Compounds* 16(5), 552–556.
19. Estevez-Fregoso E., Farfán-García E D., García-Coronel I H., Martínez-Herrera E., Alatorre A., Scorei R. I., Soriano-Ursúa M. A. (2021). Effects of boron-containing compounds in the fungal kingdom. *Journal of Trace Elements in Medicine and Biology* 65, 126714.
- 20.Mehedintu C., Bratila E., Cirstoiu M., Petca A., Brinduse L. A., Berceanu C. (2019). Evaluation of effectiveness and tolerability of boric acid in the treatment of vaginal infection with Candida Species. *Rev Chim* 70, 2375–2378.
21. Istriana N., & Priadi T. (2021, November). The resistance of modified manii wood with boric acid and chitosan/glycerol and heating against fungi and termites. In IOP Conference Series: Earth and Environmental Science (Vol. 891, No. 1, p. 012010). IOP Publishing.
- 22.Huang Y., Ho W., Ai Z., Song X., Zhang L., & Lee, S. (2009). Aerosol-assisted flow synthesis of B-doped, Ni-doped and B–Ni-codoped TiO₂ solid and hollow microspheres for photocatalytic removal of NO. *Applied Catalysis B: Environmental* 89(3), 398–405.
23. Zheng, J., Liu, Z., Liu, X., Yan, X., Li, D., & Chu, W. (2011). Facile hydrothermal synthesis and characteristics of B-doped TiO₂ hybrid hollow microspheres with higher photo-catalytic activity. *Journal of Alloys and Compounds* 509(9), 3771–3776.
24. Bilgin Simsek E. (2017). Solvothermal synthesized boron doped TiO₂ catalysts: Photocatalytic degradation of endocrine disrupting compounds and pharmaceuticals under visible light irradiation. *Applied Catalysis B: Environmental* 200, 309–322.
25. Erim B., Çiğeroğlu Z., & Bayramoğlu M. (2021). Green synthesis of TiO₂/GO/chitosan by using leaf extract of *Olea europaea* as a highly efficient photocatalyst for the degradation of cefixime trihydrate under UV-A radiation exposure: An optimization study with d-optimal design. *Journal of Molecular Structure* 1234, 130194.
26. Steffy K., Shanthi G., Maroky A. S., & Selvakumar S. (2018). Synthesis and characterization of ZnO phytonanocomposite using *Strychnos nux-vomica* L. (Loganiaceae) and antimicrobial activity against multidrug-resistant bacterial strains from diabetic foot ulcer. *Journal of Advanced Research* 9, 69–77.
27. Çiğeroğlu Z., ŞahinS., Kazan E. S. (2022). One-pot green preparation of deep eutectic solvent-assisted ZnO/GO nanocomposite for cefixime trihydrate photocatalytic degradation under UV-A irradiation. *Biomass Conversion and Biorefinery* 12, 73–86.
28. Zhang W., Liu T., & Xu, J. (2016). Preparation and characterization of 10 B boric acid with high purity for nuclear industry. *SpringerPlus* 5, 1–10.
29. Mallakpour S., Dinari M., (2012). Fabrication of polyimide/titania nanocomposites containing benzimidazole side groups via sol–gel process. *Prog. Org. coatings* 75, 373–378.
30. Ahmad A.A., Alakhras L.A., Al-Bataineh Q.M., Telfah A., 2023. Impact of metal doping on the physical characteristics of anatase titanium dioxide (TiO₂) films. *J. Mater. Sci. Mater. Electron* 34, 1552. <https://doi.org/10.1007/s10854-023-10948-z>
31. Erim B., Çiğeroğlu Z., Şahin S., & Vasseghian Y. (2022). Photocatalytic degradation of cefixime in aqueous solutions using functionalized SWCNT/ZnO/Fe₃O₄ under UV-A irradiation. *Chemosphere* 291, 132929.

-
32. Harabor A., Rotaru P., Score, R. I., & Harabor N. A. (2014). Non-conventional hexagonal structure for boric acid. *Journal of Thermal Analysis and Calorimetry* 118, 1375-1384.
33. Elbeyli İY. (2015). Production of crystalline boric acid and sodium citrate from borax decahydrate. *Hydrometallurgy* 158, 19-26.
34. Li W., Liang R., Hu A., Huang Z., & Zhou YN. (2014). Generation of oxygen vacancies in visible light activated one-dimensional iodine TiO₂ photocatalysts. *RSC advances* 4(70), 36959-36966.
35. Bai, W., Zhang, Z., Tian, W., He, X., Ma, Y., Zhao, Y., & Chai, Z. (2010). Toxicity of zinc oxide nanoparticles to zebrafish embryo: a physicochemical study of toxicity mechanism. *Journal of Nanoparticle Research* 12, 1645-1654.
36. Deniz F., & Akarsu C. (2018). Operating cost and treatment of boron from aqueous solutions by electrocoagulation in low concentration. *Global Challenges* 2(5-6), 1800011.
37. Perales-Martínez I A., & Rodríguez-González V. (2017). Towards the hydrothermal growth of hierarchical cauliflower-like TiO₂ anatase structures. *Journal of Sol-Gel Science and Technology* 81, 741-749.
38. Arik B., & Karaman Atmaca OD. (2020). The effects of sol-gel coatings doped with zinc salts and zinc oxide nanopowders on multifunctional performance of linen fabric. *Cellulose*, 27, 8385-8403.
39. Gao Y., Li Y., Yao L., Li S., Liu J., & Zhang H. (2017). Catalyst-free activation of peroxides under visible LED light irradiation through photoexcitation pathway. *Journal of hazardous materials*, 329, 272-279.